Quaternary Geochronology xxx (2015) 1–6

Contents lists available at ScienceDirect

Quaternary Geochronology

journal homepage: www.elsevier.com/locate/quageo

Dating quartz near saturation – Simulations and application at archaeological sites in South Africa and South Carolina

James K. Feathers [a, *], Vasilis Pagonis [b]

[a] University of Washington, Department of Anthropology, Box 353412, Seattle, WA 98195-3412, USA
[b] McDaniel College, Department of Physics, Westminster, MD 21157, USA

ARTICLE INFO

Article history:
Received 16 October 2014
Received in revised form
24 December 2014
Accepted 26 December 2014
Available online xxx

Keywords:
Quartz OSL
Single-grains
Saturation
Fast ratio
Decay constants

ABSTRACT

Single-grain dating of quartz near saturation is shown to have the potential of under-estimating equivalent dose. Experimental work shows that dose recoveries can be under-estimated when the administered dose approaches saturation, an observation also seen by Duller (2012). Duller (2012) found that by calculating the ratio between the fast and medium bleaching components, the "fast ratio", for each grain, the under-estimation can be corrected by removing those grains with low fast ratios. Similar results are shown for samples from archaeological sites in South Africa and South Carolina. To understand why grains with low fast ratios might lead to equivalent dose under-estimation, simulations using a comprehensive quartz model was employed. It was found that large grain-to-grain variation in the decay constants for the fast and medium components can cause this effect.

1. Introduction

The optically stimulated luminescence (OSL) signal from quartz is known to saturate at a lower dose level than the signal from feldspar. Dose response data are commonly fit to a saturating exponential function of the form:

$$I = I_0(1 - \exp^{(-D/Do)}) \quad (1)$$

where I is the luminescence intensity, I_0 is the intensity at saturation, D is dose, and D_0 is the characteristic dose where the intensity is (1–1/exp) times the saturation value. Wintle and Murray (2006) report D_0 values as low as 55 Gy and recommend that equivalent dose (D_e) values of more than $2D_0$ should be rejected because of high uncertainty.

Age under-estimations of quartz samples close to saturation have been reported (e.g., Lowick and Preusser, 2011), and Duller (2012) has studied the behavior of single-grain quartz close to saturation. A common symptom of older samples is a large number of grains rejected because the natural signal does not intersect a saturating regeneration growth curve. In some cases, this has been attributed to dose quenching (e.g., Bailey, 2004), but Duller (2012) notes that this can also happen, using the single-aliquot regeneration (SAR) method (Wintle and Murray, 2006), when the Lx/Tx ratio drops even though the luminescence signal (Lx) continues to increase at higher doses. This is because Lx begins to saturate while the signal from smaller test doses (Tx) does not. Because the sensitivity of the test dose increases faster than the sensitivity of the regeneration doses, this may force the growth curve to increase more slowly with dose or even to begin to go down (Duller, 2012).

Duller (2012) found from using dose recovery tests on a sample from Zambia that large administered doses were under-recovered. This under-estimation could be corrected, however, by eliminating grains with a low "Fast Ratio" (Durcan and Duller, 2011), which is the ratio between a fast bleaching signal and a slower bleaching signal. This is further examined in this paper on two sets of archaeologically-related samples that appear close to saturation: from three Middle Stone Age sites in South Africa and from sand deposits around small lakes (Carolina Bays) in coastal South Carolina.

2. Samples

Samples used in this study are listed in Supplementary Table 1. The three sites from South Africa – Diepkloof and Hollow Rock Shelter from the western Cape Province and Kathu Pan 6 from the

* Corresponding author.
E-mail address: jimf@u.washington.edu (J.K. Feathers).

http://dx.doi.org/10.1016/j.quageo.2014.12.008
1871-1014/

northern Cape Province – are described in detail in Feathers (2015). All three have Middle Stone Age occupations dating from about 60 to 80 ka. The samples from South Carolina are from sand deposits surrounding Carolina bays, which are upland ponds formed during the Late Pleistocene along the Atlantic coastal plain. While shallower deposits contain archaeological material, the samples of concern here are from deeper deposits and not associated with artifacts. Measurement procedures for both are given in Feathers (2015). To the extent different preheats may affect the results, we note that the South African samples were subjected to variable preheats between 220 and 260 °C, with no significant difference in dose recovery or D_e.

3. Fast ratio

The Fast Ratio is the ratio of intensities from two integrated portions of the decay curves: one from the fast-bleaching component and one from the medium bleaching component. To determine where on the decay curves these are best distinguished, two exponential components were fit to decay curves obtained on single grains of quartz from Diepkloof with a 4 s stimulation at 40% power, using the fitting program in Risø Analyst 4.12. Adding a third component did not improve the fit for all but a few grains. From these fits, a *b* value, which is the product of the photo-ionization cross-section (cm^2) and the stimulation light intensity (photons s^{-1} cm^{-2}), was calculated (Fig. 1). The rate of optical eviction of charge is a function of *b*. The values obtained, on average, were $10.3 \pm 3.4\ s^{-1}$ for the fast component and $2.1 \pm 0.7\ s^{-1}$ for a "slower"component, similar to those obtained by Duller (2012), 11.1 ± 4.3 and 1.94 ± 1.0, respectively. Using these numbers to determine the integrals for the ratio is complicated, partly because the effective power the laser delivers to single grains is poorly known. For these samples we obtained integrals by scaling to Duller's data according to the difference in power used for the original measurements (90% instead of 25%). The integrals for the fast component were the first channel, corresponding to 0.02 s, and for the slower component, 0.18–0.22 s, identical to those obtained in another study by Jacobs et al. (2013), who also used 90% power.

4. Dose recovery – fast ratio plateau

In dose recovery experiments, Duller (2012) found that for given doses more than about 70 Gy, the recovered dose on average systematically underestimated the given dose with high over-dispersion. By restricting analysis to those grains with Fast Ratios greater than 20, the underestimation was reduced and the over-dispersion approached zero. For all five South African samples, dose recovery tests were done using administered doses of 80 Gy (n = 241) and 40 Gy (n = 245). Before giving the dose, grains were set to zero by exposure to the 532 nm laser for one second at 125 °C. The recovered doses from the 80 Gy dose were on average about 60 Gy (Supplementary Table 2). By sequentially removing grains with the lowest fast ratios, the recovered dose/administered dose ratio increased to a plateau near 1 after a fast ratio of 2 (Fig. 2). For the 40 Gy dose the recovered/administered ratio forms a plateau near one for all fast ratios. Over-dispersion also goes down as grains with lower fast ratios are removed (Fig. 3), more dramatically for the 80 Gy than 40 Gy given dose, but not to zero as in Duller (2012). This is probably because the minimum fast ratio of 20 that Duller used could not be reached for these samples without severely reducing sample size. For the South Carolina samples, a 40 Gy dose was given, and the ratio of given to recovered was within 2σ of 1 for all three samples (Supplementary Table 2). The implication is that at higher doses, the SAR protocol may be underestimating the dose, and thus the age.

5. Sample results

Fig. 4 shows, for the South African and South Carolina samples, the change in equivalent dose (determined by the central age model) as grains with lower fast ratios are progressively removed. For all but the Herndon Bay samples, the D_e increases until a fast ratio of between 1.5 and 4 is achieved, after which removal of more grains did not change the D_e value. The Herndon Bay samples, despite having about 1 in 3 grains rejected because the natural did not intersect the regeneration curve, do not apparently suffer from potential underestimation. The over-dispersion is also reduced when low fast ratio values are excluded (Fig. 5). This indicates that grains with low fast ratios are preferentially associated with low D_e values, increasing the spread in the distribution. Low D_E values are also associated with low D_O values, as might be expected (Fig. S1), although the relationship disappears at higher D_O values, suggesting that removing grains with D_e values more than $2D_O$ does not bias against older grains. Lower D_O values, however, do not appear to be predictors of low fast ratios (Fig. S2).

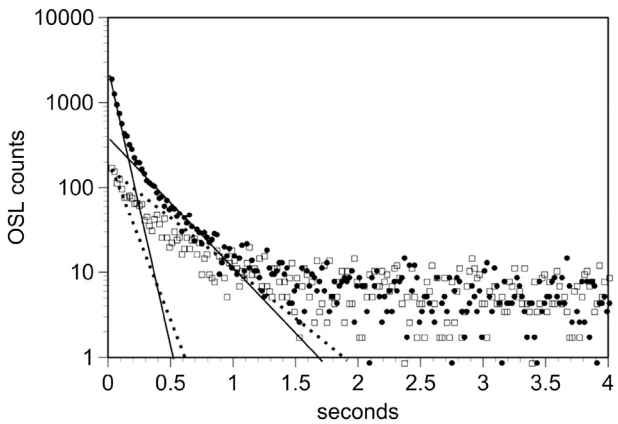

Fig. 1. Decay curves for two single grains from UW247. Filled circles, decay dominated by first component (83%); open squares, decay less dominated by first component (57%). Solid lines are fits to first and second component for the circle decay; dotted lines are fits to first and second components for the square decay.

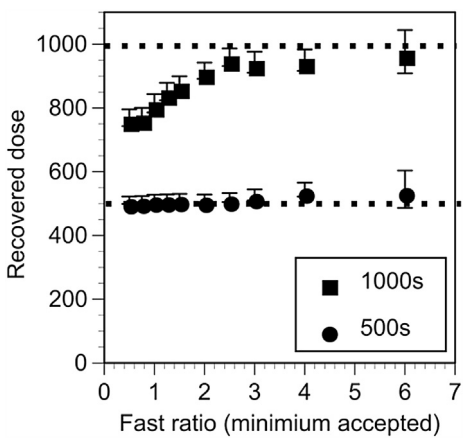

Fig. 2. Average recovered dose (in s β with 1 s β ~ 0.08 Gy), using the central age model, as a function of a minimum acceptable Fast Ratio. Box is administered dose. Dotted lines represent exact recovery. Data are from the South African samples.

Please cite this article in press as: Feathers, J.K., Pagonis, V., Dating quartz near saturation – Simulations and application at archaeological sites in South Africa and South Carolina, Quaternary Geochronology (2015), http://dx.doi.org/10.1016/j.quageo.2014.12.008

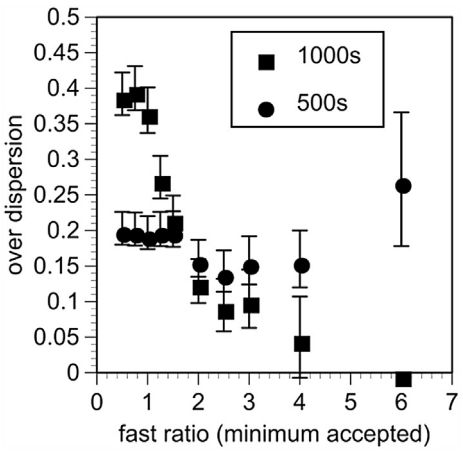

Fig. 3. Dose recovery over-dispersion as a function of minimum acceptable Fast Ratio. Box is administered dose. Data from South African samples.

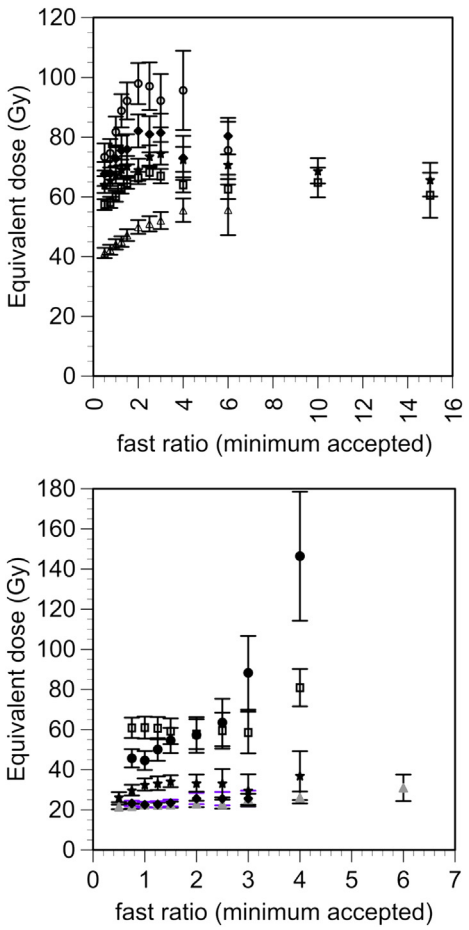

Fig. 4. Equivalent dose, from central age model, as a function of minimum accepted Fast Ratio for (top) South African samples (UW247 = square, UW260 = circle, UW264 = triangle, UW287 = diamond, UW325 = star) and (bottom) South Carolina samples (UW2730 = square, UW2731 = circle, UW2786 = triangle, UW2787 = diamond, UW2788 = star).

6. Ages

Supplementary Table 1 compares ages calculated both using all grains with acceptable signals and using only those grains with fast ratios greater than 1.5–4, depending on the sample. By removing grains with low fast ratios, the ages are increased for all samples, although not significantly for many of them.

The lack of significant difference is partly due to use of the largest component from the finite mixture model as the basis for age for most samples. (This was used to look at the structure of the broad distributions. The over-dispersion (σ_b) from dose recovery was used to constrain the variation expected for single-aged components. A smaller σ_b was used for analysis after grains with low fast ratios were removed, because the dispersion in dose recovery was less.) For example, for UW287, where the ages with and without the fast ratio criterion are nearly identical, the finite mixture model assigned 76% of the grains to the largest component when all data were considered, but 92% when just the grains with fast ratios more than 2 were considered. In the former case, the low equivalent dose values were placed in a low value component. This nearly disappeared with the high fast ratio data, where the sample is nearly single-aged. For comparison, the age from the central age model is 52.5 ± 4.8 ka for all data and 63.5 ± 7.0 for grains with fast ratios over 2. If low fast ratios are preferentially distributed among lower equivalent dose values, those might be segregated into a lower age component that is not considered for the depositional age. The real advantage of using the fast component as a criterion for rejection therefore is the lower over-dispersion, the point also

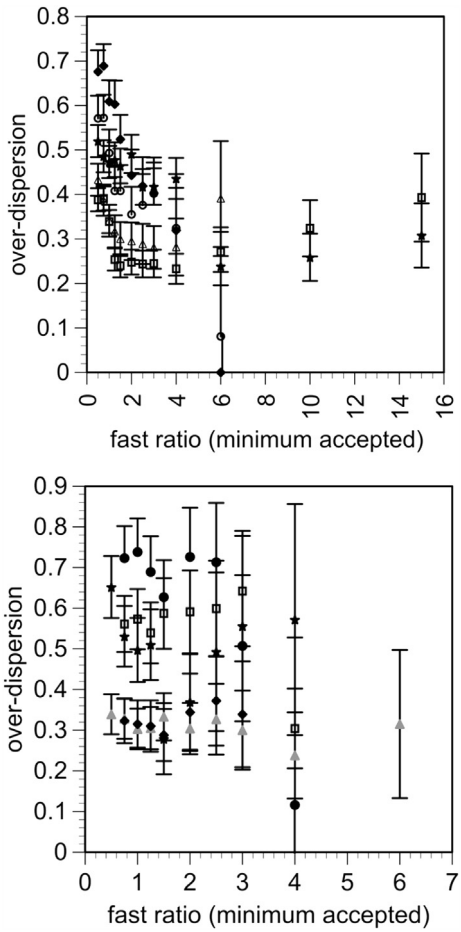

Fig. 5. Over-dispersion as a function of minimum accepted Fast Ratio for (top) South African samples (UW247 = square, UW260 = circle, UW264 = triangle, UW287 = diamond, UW325 = star) and (bottom) South Carolina samples (UW2730 = square, UW2731 = circle, UW2786 = triangle, UW2787 = diamond, UW2788 = star).

Please cite this article in press as: Feathers, J.K., Pagonis, V., Dating quartz near saturation – Simulations and application at archaeological sites in South Africa and South Carolina, Quaternary Geochronology (2015), http://dx.doi.org/10.1016/j.quageo.2014.12.008

made by Duller (2012), and therefore less risk of giving undue weight to low value components.

7. Simulations

To study why grains exhibiting a low fast ratio preferentially underestimate the dose, we performed two sets of simulations using the comprehensive quartz model described in Pagonis et al. (2008; 2011a,b). The model consists of a total of 11 electron traps and hole centers, and has been used successfully to simulate a wide variety of TL and OSL phenomena in quartz. Levels 3 and 4 in this model are of particular relevance in the experiments described in this paper, since they correspond to the fast and medium OSL components in quartz. The simulations also represent a first effort to incorporate the experimentally observed large variations of the decay constants b_{FAST} and b_{MEDIUM} in a quartz model, with the purpose of simulating the results of single grain experiments.

In a first set of simulations, a typical SAR protocol is simulated according to the procedure described in Pagonis et al. (2011a; 2011b) and shown in Supplementary Table 3. The model simulates a natural quartz sample which is optically bleached in the laboratory, followed by a laboratory irradiation with a dose in the range 20–120 Gy, and finally undergoing a standard SAR protocol to recover the given dose.

The variability in OSL characteristics of quartz is simulated by assuming that all the fundamental transition probabilities in the model remain constant, while all trap and center concentrations are allowed to vary randomly within a certain percentage from the values in the model. The parameters of the comprehensive model of Pagonis et al. (2011a) are used as a "standard" quartz model, and N = 200 versions of the parameters are generated by randomly selecting concentration values within ±20% of the original values, using uniformly distributed random numbers. This technique allows a simulation of natural variations that may occur within the same sample (Pagonis et al., 2011a,b). The optical decay constants b_{FAST} and b_{MEDIUM} of the fast and medium OSL components are not varied in this first set of simulations, in order to study just the effect of the 20% random variations in concentrations.

The OSL signal in the simulations is deconvoluted using two exponential components plus a background, and the fast ratio is calculated in two different ways. In the first method the integration intervals are taken as in the single grain experiments described in this paper, i.e. the first channel (0.02 s) is used for the fast OSL component, and the interval around 0.20 s is used to define the intervals for the medium component. In the second method used to find the fast ratio, the time at which the fast component drops to 1% of its numerical value is calculated, and this time is used to define the two integration intervals (Duller, 2012). These two methods give very similar results, and the results of the simulated fast ratios are found to be rather insensitive to the exact method used to calculate the fast ratio values. (In the experimental work, a second interval at around 0.4 s was also applied, with very similar results.)

The results (Fig. 6) for given doses between 40 and 120 Gy show that the recovered SAR doses are independent of the values of the fast ratio, and they are within 0.9–1.0 interval for the ratio with the given doses. Furthermore, all recycle values and zero dose values in these simulations are found to be within acceptable ranges. It is noted that the simulated values of the fast ratio in Fig. 6 are larger than 5 (FR > 5) for all N = 200 grains simulated in this first group of simulations. A typical distribution of the fast ratio values from this first set of simulations is shown in Supplementary Fig. S3 for a given dose of 80 Gy.

In a second set of simulations the experimentally seen wide variations of the optical decay constants b_{FAST} and b_{MEDIUM} are incorporated in the model in the form of two Gaussian distributions. The distributions have centers at 10.3 and 2.1 (s^{-1}), and corresponding widths of 3.4 and 0.7 (s^{-1}), as shown in Supplementary Fig. S4. The simulations in Fig. 6 were then repeated for N = 200 grains with the values of b_{FAST} and b_{MEDIUM} for each grain chosen randomly from these Gaussian distributions. The OSL signals are again deconvoluted in two exponential components plus a background, and the fast ratio is calculated in two different ways as previously described.

Fig. 7 shows the results of this second set of SAR simulations for the N = 200 grains, and for given doses between 40 and 120 Gy. The results in Fig. 7 are similar to the underestimation of the given doses at low fast ratios, as shown in the experimental data of Fig. 2. At low given doses <50 Gy the SAR protocol gives the same result independently of the value of the fast ratio of the grains. At higher doses >50 Gy the simulated data reproduces qualitatively the dose underestimation effect shown in Fig. 2 of this paper.

The purpose of the simulations in Figs. 6 and 7 is to demonstrate the phenomenon of underestimation of the dose at low FR values, and to investigate the possible underlying mechanism. The phenomenon of dose underestimation is clearly demonstrated in Fig. 7, and there is some improvement in the dose estimation when the minimum FR increases in Fig. 7, but the magnitude of this improvement is of the order of 2%. Therefore one sees mostly a qualitative agreement between Figs. 2 and 7, and the simulated 2%

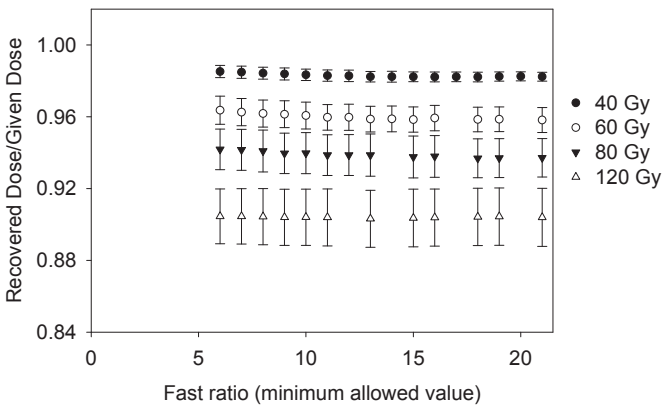

Fig. 6. The results of a first set of simulations, using a 20% variation in all trap and center concentrations, as discussed in the text. Results of the SAR simulations for the N = 200 grains, and for given doses between 40 and 120 Gy. No fast ratio values FR < 6 are present in the 200 simulated variants of the model. The error bars indicate the standard deviations of the average ratios of recovered/given dose.

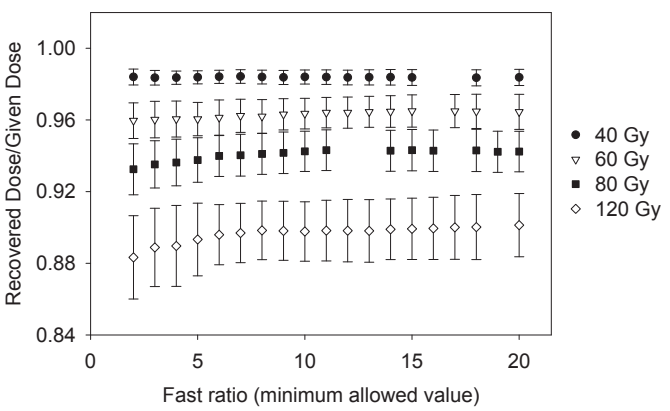

Fig. 7. The simulations in Fig. 1 are repeated using the Gaussian distributions for the decay constants, as described in the text.

Please cite this article in press as: Feathers, J.K., Pagonis, V., Dating quartz near saturation – Simulations and application at archaeological sites in South Africa and South Carolina, Quaternary Geochronology (2015), http://dx.doi.org/10.1016/j.quageo.2014.12.008

improvement in dose estimation is much smaller than the improvement one sees in the real experiment in Fig. 2. Further simulation work is necessary to clarify these quantitative differences between simulation and experiment.

Supplementary Fig. S5 shows the histogram distribution of the fast ratio values from this second set of SAR simulations at a high given dose of 80 Gy. The distribution in Supplementary Fig. S5 can be compared with the corresponding distribution of fast ratios in Supplementary Fig. S3, obtained in the first set of simulations. The former distribution is seen to be wider and more heavily shifted towards higher fast ratios, while the latter distribution is shifted towards lower FR values. The combined results in Figs. 6 and 7 indicate that the introduction of the Gaussian distributions results in lower fast ratio values, i.e. the randomness in the b_{FAST} and b_{MEDIUM} values results in a larger contribution of the medium OSL component to the simulated OSL signal.

Further evidence for the underlying mechanism causing the underestimation of the given doses is obtained by simulating the dose response of the traps corresponding to the fast and medium OSL components in quartz (levels 3 and 4 in the model of Pagonis et al., 2011a). The average dose response for the N = 200 variants is shown in Fig. 8. The error bars in this figure represent the standard errors of the average concentrations of filled traps for the ensemble of N = 200 model variants. The fast OSL trap starts saturating at doses larger than ~50 Gy, while the medium component continues to increase over the whole dose range. The dose response of both traps is almost identical for doses up to 40 Gy. Hence for given doses larger than ~40 Gy one would expect a much larger contribution from the medium OSL trap, leading to lower fast ratios.

The main physical reason the SAR protocol does not seem to respond very well to the medium component is the competition between the two traps for electrons during irradiation, as shown in the dose response curves of Fig. 8. The dose response of both traps is almost identical for doses up to 40 Gy, so one may expect similar responses of the two traps to the SAR protocol for low doses. For doses larger than ~40 Gy the fast trap starts saturating and therefore the medium trap dominates in the competition process during irradiation, with most electrons being trapped in it rather than in the fast trap. This competition effect will also have a larger effect during the subsequent heating and OSL stages of the SAR protocol, leading to inaccuracies in the experimental separation of the two components.

As the doses increases, so does the competition between the two traps, and separation of the two components experimentally becomes more difficult. The FR basically provides a quantitative measurement of the degree of competition between the two traps.

In addition to these considerations which are based on the simulations of Fig. 8, there is also the additional experimentally induced variation in the eviction power (b-values) for the two traps. This experimental variation is likely due to experimental factors like fluctuations in the laser output, alignment of the laser beam, geometrical positioning of the grains etc.

Supplementary Fig. S6 shows the average simulated L/T signals for the N = 200 variants in the model, for the two sets of simulations carried out in this paper. Fig. S6(a) shows the L/T results for the first set of simulations based only on the 20% variations of concentrations, while Fig. S6(b) shows the resulting L/T dose response when the two Gaussian distributions are included for b_{FAST} and b_{MEDIUM}. Both L/T dose responses in Fig. S6 are seen to have very small error bars up to doses of ~70 Gy. However, Fig. S6(b) shows clearly that for larger doses the introduction of the Gaussian distributions results in large possible ranges of the dose responses. This large possible range of L/T responses could then lead to large variations in the recovered doses from the SAR protocol.

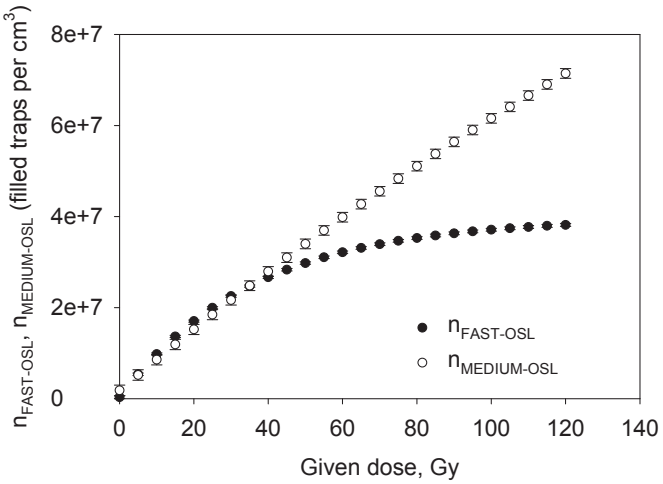

Fig. 8. Simulated average dose responses of the traps corresponding to the fast and medium OSL components in quartz, for the N = 200 variants in the model. The fast OSL trap starts saturating at doses larger than ~50 Gy, while the medium component continues to increase over the whole dose range. However, the dose response of both traps is almost identical for doses up to 40 Gy.

8. Conclusions

In dose recovery experiments with single-grain quartz, using administered doses approaching the saturation limit can result in under-estimation of the dose for grains with a significant contribution from the medium bleaching component. D_e determinations on single grains from natural samples, where the accumulated dose is close to saturation, may also lead to age under-estimation, as demonstrated by the examples in this paper. Simulations show that this can be caused by large variations in *b* values, or decay constants, for the fast and medium bleaching components. Removing grains with low fast ratios, or those with significant contributions from the medium component, can eliminate this effect and also reduce over-dispersion.

Acknowledgments

Collection and dating of samples were made possible by the Louis Leakey Foundation, the National Science Foundation, and the South Carolina Institute of Archaeology and Anthropology, University of South Carolina. Thanks also to Geoff Duller, Julie Durcan and Zenobia Jacobs for advise on calculating the fast ratio.

Appendix A. Supplementary data

Supplementary data related to this article can be found at http://dx.doi.org/10.1016/j.quageo.2014.12.008.

References

Bailey, R.M., 2004. Paper I – simulation of dose absorption in quartz over geological timescales and its implications for the precision and accuracy of optical dating. Radiat. Meas. 38, 299–310.

Duller, G.A.T., 2012. Improving the accuracy and precision of equivalent doses determined using the optically stimulated luminescence signal from single grains of quartz. Radiat. Meas. 47, 770–777.

Durcan, J.A., Duller, G.A.T., 2011. The fast ratio: a rapid measure for testing the dominance of the fast component in the initial OSL signal from quartz. Radiat. Meas. 46, 1065–1072.

Feathers, J.K., 2015. Luminescence dating at Diepkloof Rock Shelter – additional data. J. Archaeol. Sci. (submitted for publication).

Jacobs, Z., Hayes, E.H., Roberts, R.G., Galbraith, R.F., Henshilwood, C.S., 2013. An improved OSL chronology for the Still Bay layers at Blombos Cave, South Africa: further tests of single-grain dating procedures and a re-evaluation of the timing of the Still Bay industry across southern Africa. J. Archaeol. Sci. 40, 579–594.

Lowick, S.E., Preusser, F., 2011. Investigating age underestimation in the high dose region of optically stimulated luminescence using fine grain quartz. Quat. Geochronol. 6, 33–41.

Pagonis, V., Chen, R., Kitis, G., 2011a. On the intrinsic accuracy and precision of luminescence dating techniques for fired ceramics. J. Archaeol. Sci. 38, 1591–1602.

Pagonis, V., Baker, A., Larsen, M., Thompson, Z., 2011b. Precision and accuracy of two luminescence dating techniques for retrospective dosimetry: SAR-OSL and SAR-ITL. Nucl. Instrum. Methods Phys. Res. B 269, 653–663.

Pagonis, V., Wintle, A.G., Chen, R., Wang, X.L., 2008. A theoretical model for a new dating protocol for quartz based on thermally transferred OSL (TT-OSL). Radiat. Meas. 43 (2–6), 704–708.

Wintle, A.G., Murray, A.S., 2006. A review of quartz optically stimulated luminescence characteristics and their relevance in single-aliquot regeneration dating protocols. Radiat. Meas. 41, 369–391.

Please cite this article in press as: Feathers, J.K., Pagonis, V., Dating quartz near saturation – Simulations and application at archaeological sites in South Africa and South Carolina, Quaternary Geochronology (2015), http://dx.doi.org/10.1016/j.quageo.2014.12.008